Titanium parts by powder injection moulding of TiH_2-based feedstocks

E. Carreño-Morelli[1], W. Krstev[1], B. Romeira[1], M. Rodriguez-Arbaizar[1], H. Girard[1], J.-E. Bidaux[1], S. Zachmann[2]

[1]Design & Materials Unit, University of Applied Sciences Western Switzerland, CH-1950 Sion
[2]Nabertherm GmbH, 28865 Lilienthal, Germany

Titanium parts have been processed from feedstocks composed of titanium hydride powders, low density polyethylene, paraffin wax and stearic acid. A two-step debinding process has been used, which consists of solvent debinding in heptane at 50°C followed by thermal debinding at 500°C. Sintering was performed at 1200°C. Both thermal debinding and sintering were performed under a protective atmosphere in a MIM furnace equipped with molybdenum heating elements and a debinding retort. Special care in powder handling, feedstock preparation, debinding and sintering atmospheres, allowed to limit the residual oxygen, nitrogen and carbon contents, which were determined by quantitative analysis. The mechanical properties of net-shape sintered parts were measured by tensile tests. A tensile strength of 580 MPa and an elongation of 1.8% were obtained. Experimental watch bracelet segments were injection moulded, showing good shape preservation and reproducibility.

Introduction

The excellent properties of titanium and titanium alloys have been extensively reported, as well as the complex processing steps, which are currently necessary for the production of engineering parts with these materials [1]. As a consequence, the interest of producers and end-part users on net-shape technologies is growing. Recently, considerable progress in powder injection moulding of titanium and its alloys has been accomplished [2-6]. This is due to the advances in production of good quality base-powders, binders and sintering facilities. However, cost of raw materials, especially for gas atomised powders, is still a limiting factor for a number of applications. In this work, net-shape manufacturing of titanium parts has been performed by powder injection moulding from titanium hydride powders, which have the attractiveness of being less reactive than fine titanium powders, easier to handle, and cheaper [7-8].

Experimental

Raw materials and feedstock processing

Two types of TiH_2 powders from AG Materials Inc., Taiwan, were used: a fine TIH-25AA grade (D_v50 = 9.43 µm) and a coarse TIH-020A grade (D_v50 = 19.52 µm). The angular morphology of these powders can be seen in Fig. 1. The scanning electron microscopy observations were performed in a LEO1525 microscope.

The particle size distribution was determined by laser diffractometry in a Malvern Mastersizer 2000 apparatus. Table 1 presents the particle size parameters D_v10, D_v50 and D_v90 as well as the volume moment mean diameter D [4,3]. The specific surface area is estimated as $SSA=6/(\rho.D[3,2])$, where D [3,2] is the surface area moment mean diameter and $\rho = 3.9$ g/cm^3 is the density of TiH_2.

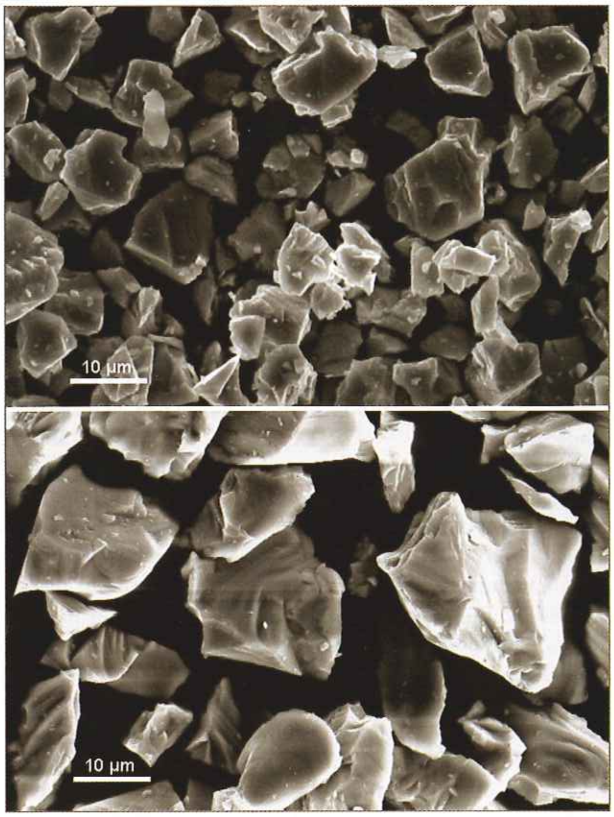

Fig. 1 Scanning electron microscopy of starting TiH_2 powders: fine TIH-25AA (top) and coarse TIH-020A (bottom)

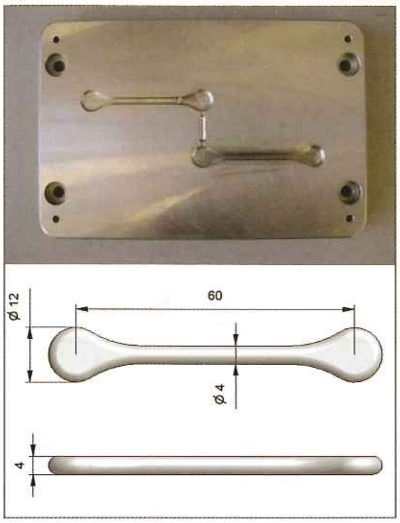

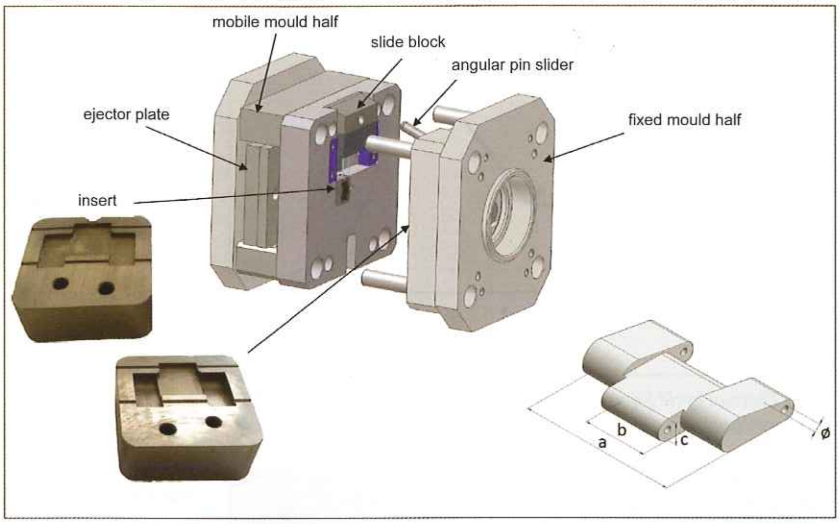

Fig. 2 Mould half for tensile test specimen and dimensions of the mould cavity in mm

Fig. 3 Tool set (mould frame, inserts, slide) and drawing of watch bracelet segment

The binder consisted of 55 wt% paraffin wax (Fluka Chemie GmbH, Buchs, Switzerland), 35 wt% low density polyethylene (LDPE Riblene MP30, Polimeri Europa, Italy) and 10 wt% stearic acid (Fluka Chemie GmbH). The binder volume fraction was 40 vol%. Feedstocks for powder injection moulding were prepared in a Coperion LUK 1.0 sigma blade mixer (Werner & Pfleiderer, Stuttgart, Germany). Mixing was performed at 140°C for 4h. Then, polymer-powder granules were obtained by cooling down and crushing the mixture by slow shearing.

Injection moulding

Tensile test specimens (Fig. 2) and experimental watch bracelet segments were injection moulded in an Arburg 221K 350-100 machine (Arburg GmbH + Co KG, Lossburg, Germany).

The mould for watch bracelet segments (Fig. 3) consists of single cavity inserts in a mould frame. A slide block with two pins is mounted on the mobile mould half. An angular pin slider in the fixed mould half forces motion of the slide block when the mould closes. It allows transverse holes along the parting line to be obtained for further assembly of the segments to each other. Mould temperature was about 40°C.

Debinding and sintering

After shaping, the parts were subjected to successive treatments of solvent debinding, thermal debinding, dehydrogenation and sintering.

Solvent debinding was performed in heptane at 50°C for 10 h, which allowed the removal of more than 98% of paraffin wax and stearic acid.

Thermal debinding, dehydrogenation and sintering steps were accomplished in a single thermal cycle in a Nabertherm VHT8-16MO MIM furnace, which is equipped with molybdenum heating elements and a debinding retort (Fig. 4). The furnace design allows safe evacuation of products resulting from binder burnout without contaminating the heating elements. During debinding, a gas flow is currently activated into the furnace chamber, and gas aspiration is directly made from the retort. During sintering, the gas flow is activated into the retort, and aspiration is made from the furnace chamber. A binder trap, which is periodically cleaned, avoids contamination of the vacuum pump. Thermal cycles can be done under vacuum or controlled atmosphere of Ar, N_2 or H_2. Fig. 4 shows details of the furnace chamber and retort.

Thermal decomposition of the LDPE backbone polymer was accomplished during a debinding step of 1 h at 500°C under argon (Fig. 5). A gas flow of 100 l/h is used for a continuous renewal of the debinding atmosphere.

Thermogravimetric analysis of TiH_2 powders performed in a Setaram TAG 24 device allowed to establish that 500°C is also an appropriate temperature for dehydrogenation. Hydrogen removal proceeds during the subsequent heating to reach the sintering temperature. At about 700°C, dehydrogenation is completed. Sintering was performed at 1200°C for 1h under flowing argon.

Material characterisation

Density measurements were performed by using the Archimedes method. Mechanical properties were characterised by standard tensile tests. Metallographic preparation of sintered samples was performed by diamond polishing followed by oxide polishing with colloidal silica. Quantitative analysis was performed by fusion

TiH_2	D_v10 [µm]	D_v50 [µm]	D_v90 [µm]	D [4,3] [µm]	SSA [m²/g]
TIH-25AA	4.72	9.43	17.01	10.18	0.21
TIH-020A	10.30	19.52	34.43	21.10	0.09

Table 1 Particle size parameters and specific surface area of fine and coarse TiH_2 powders

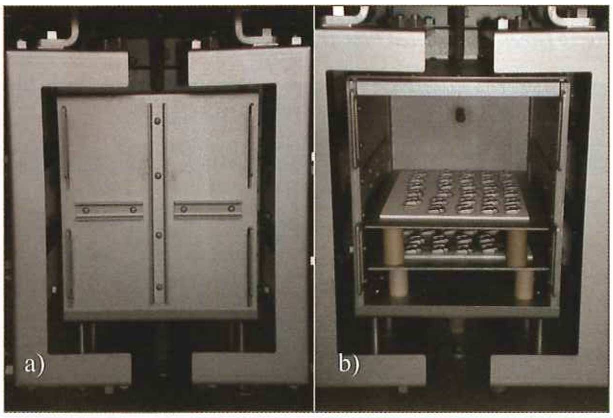

Fig. 4 Details of the debinding and sintering furnace: (a) heating elements and debinding retort closed, (b) sintered watch bracelet segments on zirconia coated alumina support, placed on molybdenum plates inside the retort

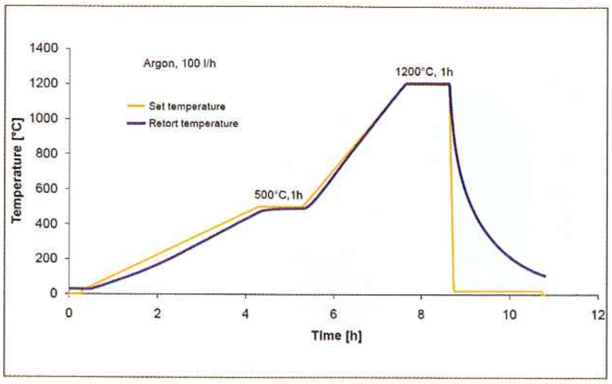

Fig. 5 Thermal cycle for processing Ti parts from solvent debinded TiH_2 based feedstocks

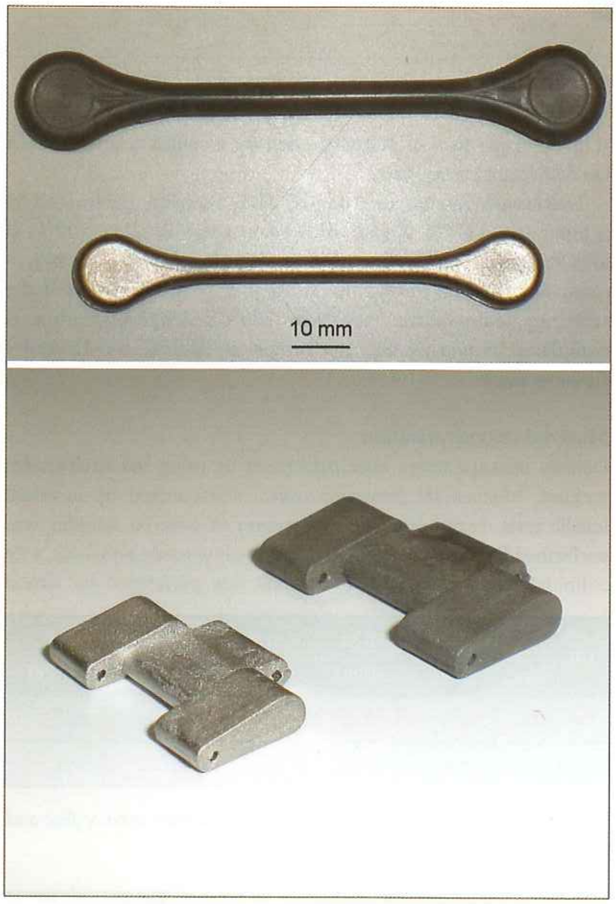

Fig. 6 Green and sintered PIM-Ti parts

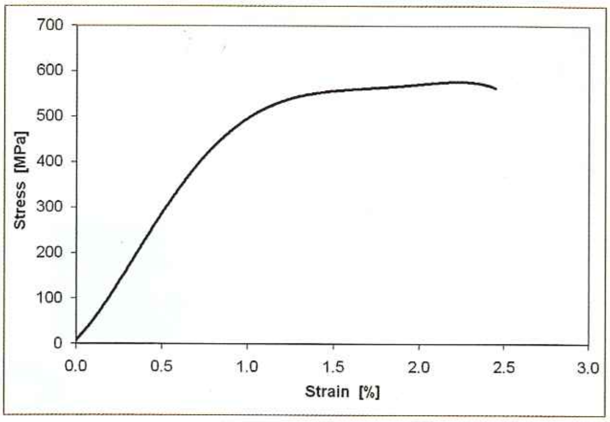

Fig. 7 Tensile stress-strain curve of sintered PIM-Ti (coarse powder)

and infrared detection with a LECO TC500 system to establish the content of interstitial elements O, N, C in base powders and sintered parts.

Results and discussion

Fig. 6 shows green parts (as injected) and net-shape parts (after debinding and sintering). Good green strength is due to low density polyethylene, which is the backbone polymer of the multicomponent binder. The goal of the solvent debinding step is to remove paraffin wax and stearic acid, leaving an open porosity to allow proper thermal debinding of the backbone polymer. In this way, gas bubble formation during polymer burnout is avoided, reducing internal stresses and the risk of part damage or geometry distortion.

The linear shrinkage of sintered titanium parts is about 19%. This high value is because, in addition to the current contraction during debinding, there is also a contraction during the dehydrogenation of the TiH_2 base powder.

PIM titanium parts from fine TIH-25AA powders have a density higher than 98% of the theoretical density and tensile strength of 650 MPa, but low ductility (Table 2). This is related with the too high oxygen content, about 60 wt.%, which was measured by fusion and infrared detection.

Better results are obtained with PIM titanium parts from coarse TIH-020A powders. This is related with a lower interstitial content, especially oxygen, compared with fine powders (Table 2). Coarse powders have a lower specific surface area, which results in lower reactivity and reduced contamination during production, handling and further shaping and consolidation treatments. Sintered density is lower, but ultimate tensile strength of 580 MPa meets the requirements for Ti grade 4. In addition, elongation to fracture is improved to reach 1.8 % plastic strain (Fig. 7). However, the

	D_v50 [µm]	O [wt.%]	N [wt.%]	C [wt.%]	sintered density [%]	UTS [MPa]	elongation [%]
TIH-25AA powder	9.80	0.25	0.24	0.16	-	-	-
PIM-Ti (a)	-	0.60	0.013	0.10	98.2	650	0.7
TIH-020A powder	19.55	0.07	0.14	0.013	-	-	-
PIM-Ti (b)	-	0.38	0.046	0.045	95.8	580	1.8
Ti grade 4	-	0.4	0.03	0.08		550	15

Table 2 Interstitial content and mechanical properties of base powders, titanium standard grade 4, and PIM-Ti processed from fine (a) and coarse (b) TiH_2 powders

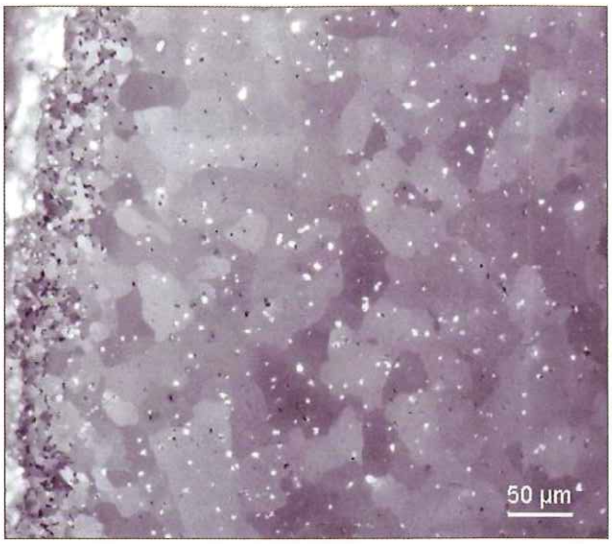

Fig. 8 Optical metallography showing the microstructure of sintered PIM-Ti (fine powder)

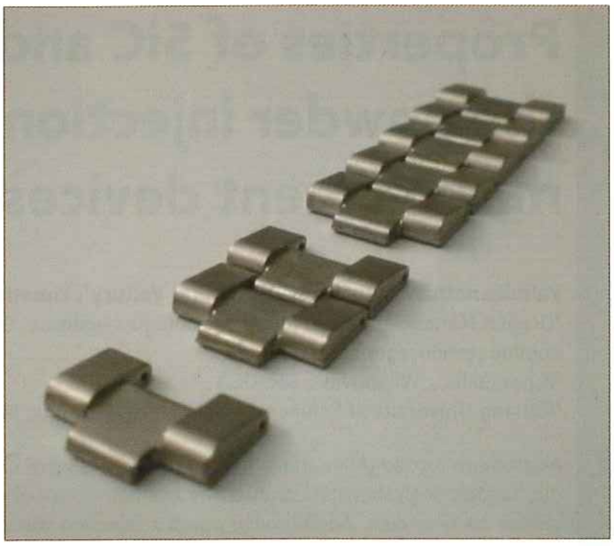

Fig. 9 Titanium watch bracelet segments processed from TiH_2 based feedstock

elongation to fracture is much less than the one of titanium grade 4. Further improvement in ductility would be possible by optimising the debinding, dehydrogenation and sintering cycle (e.g. by increasing sintering temperature and time), and by using TiH_2 powders of higher purity.

The microstructure of sintered parts is shown in Fig. 8. An equiaxed grain structure is found, with reduced grain size near the surfaces. Residual round porosity is also observed.

At the present state of research, injection moulding of TiH_2 feedstocks appears as an interesting alternative for manufacturing of lightweight strong parts, when ductility is not the critical requirement.

Sintered watch bracelet segments show good shape preservation and reproducibility. The variation in weight of green parts is less than 0.4%. The linear shrinkage is about 20%, and the hole diameter ø is reduced from 0.98 mm to 0.78 mm after sintering. A control of weight and dimensions was performed on 63 sintered parts. The variation in weight is again less than 0.4%. The scatter in dimensions a and b is about 0.4 %, and the scatter in the dimension c is about 0.5% (Fig. 3 and 9).

The parts can be surface treated by barrel finishing, etching, electropolishing and anodic oxidation (Fig. 10).

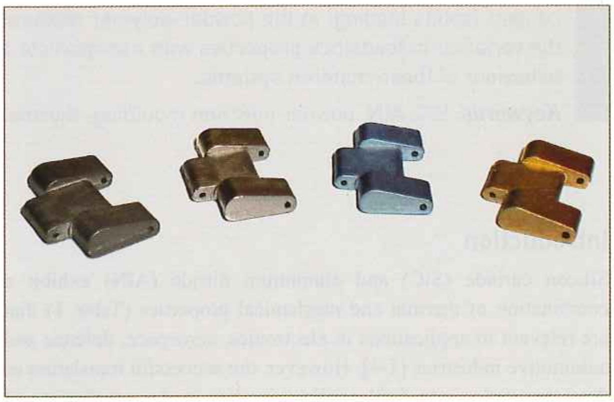

Fig. 10 Watch bracelet segments after successive surface treatments: barrel finishing (dark grey), etching and electropolishing (light grey), and anodic oxidation (blue, yellow)

Concluding remarks

Titanium hydride powders are an interesting alternative for processing PIM-Ti parts. Despite its angular shape (which is currently associated with low packing and high interparticle friction) and a necessary dehydrogenation step, sintered densities higher than 95% can be obtained. Net-shape as-sintered parts show good mechanical properties, good shape preservation and reproducibility. Further improvements in ductility will be related with the optimisation of debinding, dehydrogenation and sintering cycles, and with the availability of powders of improved purity.

Acknowledgments

The authors would like to thank A. Moreillon and G. Follonier for their help in mould design. The technical support of A. Steiner, D. Zufferey, H. Hamdan (HES-SO Valais) and J. Dänzer (BFH-Biel) is gratefully acknowledged.

References

[1] M. J. Donachie, *"Titanium, a technical guide"*, 2nd Edition, ASM International, Materials Park, Ohio, 2000

[2] Y. Itoh, T. Harikou, K. Sato, H. Miura, *Proc. of PM2004 Powder Metallurgy World Congress*, Vienna, Austria, 17-21 October 2004, pp. 445-450

[3] F. H. Froes, *Metal Powder Report*, 61, 11, 2006, pp. 20-23

[4] T. Ebel, *PIM International*, 2, 2, 2008, pp. 21-30

[5] R. Zhang, J. Kruzewski, J. Lo, *PIM International*, 2, 2, 2008, pp. 74-78

[6] R. M. German, *PIM International*, 3, 4, 2010, pp. 21-37

[7] E. Nyberg, M. Miller, K. Simmons, K. Scott Weil, *Mat. Sc. Eng.* C 25 (2005) pp. 336-342

[8] Y. Li, X.M. Chou, L. Yu, *Powder Metallurgy*, 49, 3, 2006, pp. 236-239